

## B Physics at STAR

Jens Sören Lange<sup>1</sup>, for the STAR Collaboration

<sup>1</sup> University of Frankfurt, Institut für Kernphysik,  
August-Euler-Straße 6, 60486 Frankfurt/Main, Germany

PACS: 25.75.Dw

### 1. $b$ quarks in $A+A$ collisions

In relativistic nucleus-nucleus collisions, heavy quarks ( $c, b$ ) are produced in the early stage [ 2], at time scales  $t \simeq 0.2-0.5$  fm/c, in comparison to typical pion freeze-out time scales of  $t \simeq 10$  fm/c. In particular,  $b$  quarks are interesting for two reasons:

(1) The mass of the  $c$  quark  $m(c) = 1.40$  GeV is about the same order of magnitude as  $\Lambda_{QCD} \simeq 1$  GeV, but  $m(b) = 4.75$  GeV is significantly larger. Thus, for the  $b$  quarks, pQCD based cross section predictions are more reliable than for  $c$  quarks.

(2) For  $Au+Au$  collisions at RHIC, the primordial temperature might be high enough to create  $c\bar{c}$  pairs thermally, but not  $b\bar{b}$  pairs. For  $t = 0.6$  fm/c, a temperature of  $T \simeq 0.3$  GeV can be estimated [ 3]. At such a high temperature, QCD predicts that gluons, which are massless at  $T = 0$ , acquire an effective mass, which turns out to be in the same order of magnitude as the temperature itself, i.e.  $m_{gluon} \simeq 0.3$  GeV [ 4]. Thus the production process  $gg \rightarrow c\bar{c}$  might be enhanced thermally. However, for  $b\bar{b}$  production, the Boltzmann suppression factor is  $\langle b\bar{b} \rangle / \langle c\bar{c} \rangle = \exp[-2m(b)/2m(c)] \simeq 1/23$ , thus any thermal  $b\bar{b}$  enhancement is unlikely. Thus,  $b$  quarks can be regarded as a pure probe of the early stage of the collision. However,  $b\bar{b}$  events are rare. At RHIC,  $b\bar{b}$  measurements are now feasible for first time, due to three reasons: (1) The  $b\bar{b}$  production cross section at  $\sqrt{s} = 200$  GeV (RHIC) is about a factor of  $\sim 10^3$  higher than at  $\sqrt{s} = 18$  GeV (SPS). (2) High collider luminosity provides a recorded data sample of  $10^6-10^7$  events. (3) Recent technological and price development of fast CPUs created the basis for the possibility of event reconstruction in realtime for application as high level trigger on rare events.

This paper describes the first attempt to observe  $b\bar{b}$  production with the STAR experiment at RHIC. The main STAR detector is a large scale ( $R = 2$  m,  $L = 4$  m) TPC (Time Projection Chamber) [ 1] with  $5 \times 10^7$  position pixels, each measuring the particle ionization  $dE/dx$  using a 10-bit ADC. For triggering on rare  $b\bar{b}$  events, a Level-3 trigger CPU farm was used, described in Section 4.

The  $b\bar{b}$ -bound state  $\Upsilon$  is specifically interesting, as the formation and re-breakup

rates are sensitive to color screening and thus the initial gluon density. STAR is particularly suited for the search for  $\Upsilon$  production due to its large midrapidity coverage. Because of its high mass, the  $\Upsilon$  is produced almost at rest, disfavouring gluon-boosted forward/backward emission of the decay products.

## 2. The case of the $\Upsilon$

In the following, the term  $\Upsilon$  will be used to represent the three  $S$  states  $\Upsilon(1S)$ ,  $\Upsilon(2S)$  and  $\Upsilon(3S)$ .  $\Upsilon$  properties are listed in Tab. 1. The production ratio is independent from  $\sqrt{s}$  in leading order QCD, thus ratios measured at  $\sqrt{s}=1.8$  TeV are applicable to RHIC energies ( $\sqrt{s}=200$  GeV).

	$m/\text{GeV}$	$R_{prod}$	$\text{BR}(e^+e^-)$
$\Upsilon(1S)$	9.460	72%	2.38%
$\Upsilon(2S)$	10.023	18%	1.18%
$\Upsilon(3S)$	10.355	10%	1.81%

**Table 1.** Mass  $m$  [ 5], production ratio for midrapidity  $R_{prod}$  [ 6] and branching fraction [ 5] into  $e^+e^-$ , for the lowest three  $\Upsilon$  states.

The  $\Upsilon(4s)$  and  $\Upsilon(5s)$  shall not be considered here, as they are above the  $B\bar{B}$  and  $B_s\bar{B}_s$  thresholds, respectively. All  $\Upsilon$  singlet  $^1S$ ,  $^1P$  states are still unobserved, although they are expected to exist. So far, only  $\Upsilon$  triplet states have been observed, because most data were recorded from  $e^+e^-$  annihilation ( $J^{PC}(\gamma^*)=1^{--}$ ). Recently the discovery of  $\Upsilon(1D)$  was reported [ 7], the only long-lived  $L=2$  meson ever observed. The  $\Upsilon$  decays into  $e^+e^-$  with a branching fraction of  $\simeq 2\%$  (Tab. 1). Experimentally, this is the easiest exclusive final state to measure, whereas the decay into a  $ggg$  final state (3 jets) with the largest branching fraction of 77.4% is experimentally unobservable. At  $\sqrt{s}=200$  GeV,  $\simeq 90\%$  of the  $\Upsilon$  are produced by  $gg \rightarrow b\bar{b}$ ,  $\simeq 10\%$  by  $q\bar{q} \rightarrow b\bar{b}$  ( $q$  denoting  $u, d, s$  or  $c$ ). As the total cross section for  $b\bar{b}$  production in  $p+p$  is  $\sigma(b\bar{b})=1.5 \mu\text{b}$ , one expects about one  $b\bar{b}$  pair in  $\simeq 52$   $Au+Au$  central events. With a production cross section of  $\sigma(\Upsilon)=8.4$  nb, it follows, that  $1/178$  of  $b\bar{b}$  pairs form a resonance<sup>1</sup>. A pure statistical production model, which works well for lighter particles, does not seem to be applicable [ 8]. For a rate estimate, the baseline prediction for  $\sigma_{pp}(\Upsilon)$  is taken from [ 9]. The cross section has a typical threshold behaviour  $\sigma=\sigma_o(1-m_\Upsilon/\sqrt{s})^n$ , rising steeply in the RHIC energy region. Feed-down contributions are included in the calculation, e.g. only 52% of the  $\Upsilon(1S)$  are produced directly. Feed-down contributions are 10% from the  $\Upsilon(2S)$ , 2% from the  $\Upsilon(3S)$ , 26% from the  $\chi_b(1P)$ , and 10% from the  $\chi_b(2P)$ . With an absorption correction  $\alpha$ , the fraction of the geometrical cross section  $f_{geo}$  (10% for central collisions) and the fraction of hard processes  $f_{hard}$ , the number of expected  $\Upsilon$  per one central  $Au+Au$  collision at  $\sqrt{s}=200$  GeV can be estimated as

$$\begin{aligned}
 N_\Upsilon^{Au+Au} &= BR(e^+e^-) \cdot \frac{d\sigma_{pp}}{dy} \Big|_{y=0} \cdot \frac{\Delta y \cdot \varepsilon_{rec} \cdot (AA)^\alpha \cdot f_{hard}}{\sigma_{geo} \cdot f_{geo}} \\
 &= 100pb \cdot \frac{2 \cdot 14.5\% \cdot (197 \cdot 197)^{0.95} \cdot 0.4}{7.2b \cdot 0.1} \simeq 3.7 \cdot 10^{-7}.
 \end{aligned} \tag{1}$$

<sup>1</sup>As a comparison,  $1/116$   $c\bar{c}$  pairs form a  $J/\psi$ .

### 3. Lepton Identification

Electrons were identified by their specific ionization  $dE/dx$  in the TPC, which saturates at  $dE/dx \simeq 17$ -18 keV/cm for  $p \geq 1$  GeV/c. Due to the mass dependence in the relativistic Bethe-Bloch formula, charged pions show increasing  $dE/dx \simeq 11$ -14 keV/cm for  $p=1$ -10 GeV/c. As shown in Fig. 3, for this analysis electron candidates were identified by a cut on  $dE/dx$ :

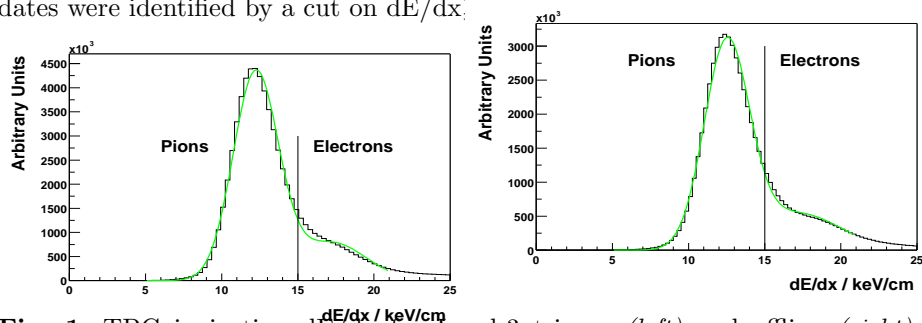


**Fig. 1.** TPC ionization  $dE/dx$  for Level-3 trigger (*left*) and offline (*right*) for  $p_T \geq 3$  GeV. For electron identification, a cut  $dE/dx \geq 15$  keV/cm was confirmed.

The observed  $e/\pi$  ratio for events with two  $p \geq 3$  GeV/c tracks is  $\simeq 1/3.5$ , determined from a two-gaussian fit (line in Fig. 1). The pion contamination in the electron sample is 17%. Imperfection of the fit in the region  $dE/dx \simeq 14$ -16 keV/cm is resulting from muon contamination, which is not taken into account for this paper<sup>2</sup>. Additional contamination from other particles (e.g. deuterons) is included in the systematic error. The electron identification was additionally checked with a partial electromagnetic calorimeter [ 10] (400 towers,  $\Delta\varphi=60^\circ$ ,  $0 \leq \eta \leq 1$ ). For  $dE/dx$ -selected electron candidates  $p/E=1.0 \pm 0.2$  was achieved.

### 4. The Level-3 Trigger

The STAR Level-3 trigger performs full-event reconstruction in realtime, utilizing both fast CPUs and a fast network. 432 Intel i960 CPUs perform TPC cluster finding, 48 ALPHA DS-10 CPUs perform TPC track finding, and 3 Intel Pentium CPUs apply global algorithms, such as invariant mass calculations. For the 10% most central  $Au+Au$  events ( $\simeq 130,000$  clusters,  $\simeq 4500$  tracks), a sustained Level-3 processing rate of  $R \leq 40$  Hz was achieved. For a solenoidal magnetic field of  $B=0.25$  T, the  $p_T$  resolution for (electron) tracks with  $p_T=5$  GeV/c was determined offline to be  $\Delta p_T/p_T \simeq 9\%$  and  $\simeq 17\%$  (with and without vertex constraint, respectively), and, on the Level-3 trigger,  $\Delta p_T/p_T \simeq 10\%$  and  $\simeq 26\%$  [ 11]. For  $B=0.5$  T, all resolutions are to be multiplied by a factor 1/3. The  $dE/dx$  resolution is offline  $\simeq 8\%$ , and on the Level-3 trigger  $\simeq 11\%$ . Further details are described elsewhere [

<sup>2</sup>For dilepton invariant mass in the high mass region, mass differences between electrons and muons are negligible, and thus, for the muon contamination, an identical invariant mass slope is expected.

11]. For the  $\Upsilon$ , the Level-3 trigger algorithm performed a trigger YES/NO decision, based upon an invariant mass cut for  $p_T \geq 3$  GeV/c and  $dE/dx \geq 15$  keV/cm selected electron candidates. The  $\Upsilon$  enhancement factor varied in the range 1.8-4.1, based on momentary accelerator luminosity conditions.

## 5. Results

The analyzed data sample is  $N_{Event}=2,400,060$  Au+Au 10% most central, additionally  $N_{Event}=212,030$  Au+Au 10% most central, triggered by the Level-3  $\Upsilon$  algorithm, and  $N_{Event}=2,309,063$  Au+Au minimum bias events. The data were taken during a period of  $\simeq 100$  days at  $\sqrt{s} = 200$  GeV. Assuming a number of 1150 binary  $p+p$  collisions per one Au+Au collision, the data set corresponds to  $\simeq 4.2 \cdot 10^9$   $p+p$  collisions. As a comparison, the amount of raw data on tape correspond to  $\simeq 10 \times$  total data sample of a recorded  $100 \text{ fb}^{-1}$   $B$  meson factory data sample. Fig. 1 shows the experimental results for the reconstructed invariant mass. A pseudorapidity cut of  $|\eta| \leq 1$  is applied. The top row shows di-electrons for unlike-sign (*left*) and like-sign<sup>3</sup> (*right*) charge pairs. The straight line represents an exponential fit to the  $m \leq 8$  GeV region, in order to visualize slope changes. The second row shows invariant mass for a control sample, i.e.  $\pi^{+-}\pi^{+-}$  candidates selected by  $dE/dx \leq 15$  keV/cm and normalized to the number of di-lepton candidates. The systematic error<sup>4</sup> consists of a  $p_T$  dependant  $\Delta p_T/p_T$  resolution, a charged pion contamination of 17%, and an additional 10% systematic uncertainty induced by cut selection. The experimental data are compared to PYTHIA 6.212 [12] calculations for the different subprocesses  $pp \rightarrow B\bar{B} \rightarrow e^+\bar{\nu}X e^-\nu X$  (*third row, left*),  $pp \rightarrow D\bar{D} \rightarrow e^-\nu X e^+\bar{\nu}X$  (*third row, right*), Drell-Yan  $pp \rightarrow e^+e^-X$  (*fourth row, left*), and  $\Upsilon$  production  $pp \rightarrow \Upsilon(1S, 2S, 3S) \rightarrow e^+e^-$  (*fourth row, right*). The expected STAR mass resolution is  $\Delta m = 340$  MeV for the  $\Upsilon(1S)$  alone, and  $\Delta m = 610$  MeV for the  $\Upsilon(1S, 2S, 3S)$  combined (non-resolvable). The PYTHIA  $k$ -factor<sup>5</sup> was set to  $k=3.0$ . GRV94L was used as the parton distribution. All simulated mass distributions are normalized to the experimental data sample (Section 5), taking into account enhancement factors on the Level-3 trigger. Two conclusions can be drawn. (1) The dilepton invariant mass distributions follow an exponential slope for  $m \leq 9$  GeV, whereas the fit line is in the following referred to as *reference line*. An enhancement above the reference is visible for  $m \geq 9$  GeV, for both unlike-sign and like-sign di-electrons. The normalized di-pion control sample shows a non-exponential slope, for  $m \geq 6$  GeV beneath the reference line. As seen from reference line comparison, any possible contamination from the di-pions cannot explain the observed enhancement of the dileptons for  $m \geq 9$  GeV. From comparison to PYTHIA, it can be concluded that the major distribution to the di-electrons results from  $B\bar{B}$  production with subsequent semileptonic decays. Drell-Yan does not contribute significantly,

<sup>3</sup>The like-sign histogram is normalized according  $2 \cdot \sqrt{N^{++} \cdot N^{--}}$ .

<sup>4</sup>All error components were summed in quadrature.

<sup>5</sup> $k$ -factor is defined as ratio of cross sections for next-to-leading-order QCD and leading-order QCD. No higher loops were taken into account.

as the cross section is small  $\sigma(q\bar{q}\rightarrow e^+e^-)\leq 10$  nb.  $D\bar{D}$  events are highly suppressed with a factor  $\simeq 10^7$  due to the electron  $p\geq 3.0$  GeV/c cut.

(2) The unlike-sign dilepton distribution seems to indicate peak-like structure in the mass region  $m\geq 9$  GeV. In order to exclude possible accidentally used  $B=0$  T events, which could fake high- $p_T$  tracks, a second independent analysis confirmed the peak structure. The peaks remain visible when using a *2-dim* (Level-3 trigger) or *3-dim* (offline) track finder algorithm, or when perform track finding with or without vertex constraint. If the peak structure was induced by  $\Upsilon$  production, it would indicate the unlikely fact, that the production cross section would be enhanced by a factor  $\simeq 10^3$  compared to the baseline prediction (Section 2). Any additional processes generating high mass di-leptons are not known.

## 6. Systematic studies of $\sigma_{pp}(\Upsilon)$ cross section prediction

The question of whether the observed peak structure might be induced by enhanced  $\Upsilon$  production was investigated by systematic variation of three different basic QCD parameters in PYTHIA 6.212.

(1) In the  $\sigma_{pp}(\Upsilon)$  calculation a fixed mass  $m(b)=4.75$  GeV is assumed, but  $m(b)$  depends on the momentum transfer  $Q^2$  in  $gg, q\bar{q}\rightarrow b\bar{b}$ , i.e.  $m(b)\simeq 4.5$  GeV for  $Q=1$  GeV/c,  $m(b)\simeq 3.5$  GeV for  $Q=10$  GeV/c,  $m(b)\simeq 3.0$  GeV for  $Q=100$  GeV/c.

(2)  $\sigma_{pp}(\Upsilon)$  also depends on the squared  $\Upsilon$  wave function at the origin  $|\Psi(r=0)|^2$ , which is calculated from the leptonic decay width

$$\Gamma(\Upsilon \rightarrow l^+l^-) = \frac{64\pi}{9} \frac{\alpha_{em}^2 e^2 |\Psi(r=0)|^2}{m_{e^+e^-}^2} \quad (2)$$

with exp. errors  $\pm 4\%(1s), \pm 16\%(2s), \pm 18\%(3s)$ .

(3)  $\sigma_{pp}(\Upsilon)$  depends on the strong coupling constant  $\alpha_s$ , which itself depends on the gluon distribution  $xG(x, Q^2(x))$ . As an example, the early stage of an  $A+A$  collision might be governed by gluon saturation, simply given by the geometrical condition, that the probability of two colliding gluons in a gluon cascade is equal to one.

$$\frac{3\pi^2\alpha_S A}{2Q_{saturation}^2} \times \frac{x \cdot G(x, Q^2(x))}{\pi R_A^2} = 1 \quad (3)$$

Additionally,  $\alpha_s$  is a function of temperature  $\alpha_s(T)\sim 1/\ln(T)$  [ 9]. At a scale of  $\sqrt{s}=\sqrt{3}$  GeV, [ 5] quotes  $\alpha_S=0.280\pm 0.035$  (expt) $\pm 0.050$  (syst) $_{-0.030}^{+0.035}$  (theory). The total (quadratically summed) error is  $\pm 0.069$ , thus  $\Delta\alpha_S/\alpha_S=25\%$ .

The variation of  $\Delta\sigma_{pp}(\Upsilon)/\sigma_{pp}(\Upsilon)$  from the baseline prediction (Ch. 2) was investigated using PYTHIA 6.212, and found to be a factor 1.0–3.0 (only an increasing effect observed) for  $m(b)$ , a factor 0.7–1.3 for  $|\Psi(r=0)|^2$ , and a surprisingly large factor of  $10^{-2}$ –1.0 (only a decreasing effect observed) for  $\alpha_S$ . However, in order to explain the observed peak structure in Fig. 1 (top, left) a  $\sigma_{pp}(\Upsilon)$ -enhancement of a factor  $\simeq 10^3$  would be needed. Thus, at this stage,  $\Upsilon$  production must be excluded as explanation. For alternative explanations, two additional effects should

be considered:

(1) A peak structure might be generated by  $B\bar{B}$  ( $m=10.56$  GeV) or  $B_s\bar{B}_s$  ( $m=10.74$  GeV) threshold effects. Both meson species decay with large branching fractions of 10.5% and 8.1%, respectively. However, due to the undetected  $\nu$  in each decay and additionally hard-to-calculate QCD threshold dynamics, the size of the effect is difficult to estimate.

(2) A  $B$  meson oscillates by second-order weak interaction into a  $\bar{B}$  according to  $\cos(\Delta mt)$ , with  $\Delta m=0.503$  ps<sup>-1</sup> [ 13]. Using a  $B$  meson lifetime of  $c\tau=462$   $\mu\text{m}$  [ 5] and a typical  $B$  meson Lorentz boost of  $\gamma=1.2$  (corresponds to  $E_{kin}(B)=1$  GeV) it can be estimated for STAR, that  $\simeq 2/3$  of all  $B$  remain a  $B$ , and  $\simeq 1/3$  oscillate into a  $\bar{B}$ . Every oscillation flips the sign of the lepton charge in the semileptonic decay, thus the oscillation could be observed in an unlike-sign/like-sign charge asymmetry vs.  $B$  meson decay vertex. Unfortunately, the STAR  $z$  vertex resolution has not been sufficient so far to resolve the oscillation.

## 7. Apex

Explanations of the observed enhancement and peak structures in the electron invariant mass distributions might only be possible with a largely increased  $Au+Au$  data sample, which will be collected in 2004. Lepton identification at STAR will be improved by an electromagnetic calorimeter with  $|\eta|\leq 2$  and  $\Delta\varphi=2\pi$  coverage. For the envisaged RHIC-2 upgrade, starting possibly from 2007, a luminosity increase for  $Au+Au$  by a factor 40 to  $\mathcal{L}=8\times 10^{27}$  cm<sup>-2</sup>s<sup>-1</sup> is planned, thus the  $\Upsilon$  production will not be a rare process anymore. Additionally a new 2-layer pixel detector is planned at STAR, using a total of  $9\times 10^7$  pixels of 20  $\mu\text{m}^2$  in area. Such a device will clearly enable an excellent measurement of  $B$  meson secondary vertices.

## References

1. STAR Collaboration, Nucl. Phys. **A661**(1999)681
2. B. Zhang et al., Phys. Rev. **C65**(2002)054909, nucl-th/0201038
3. U. Heinz, P. Kolb, Nucl. Phys. **A702**(2002)269, hep-ph/0111075
4. R. Vogt, J. Phys. **G23**(1997)1989
5. Particle Data Group, Phys. Rev. **D66**(2002)010001
6. CDF Collaboration, Phys. Rev. Lett. **88**(2002)161802
7. CLEO Collaboration, hep-ex/0207060
8. M. Gaździcki, M. I. Gorenstein, Phys. Lett. **B517**(2001)250
9. J. F. Gunion, R. Vogt, Nucl. Phys. **B492**(1997)301, hep-ph/9610420
10. T. Cormier et al., Nucl. Inst. Meth. **A483**(2002)734, hep-ex/0107081
11. J. S. Lange et al., Nucl. Inst. Meth. **A453**(2000)397
12. T. Sjöstrand et al., Comp. Phys. Comm. **153**(2001)238, hep-ph/0010017
13. BELLE Collaboration, Phys. Rev. **D 67**(2003)052004, hep-ex/0212033

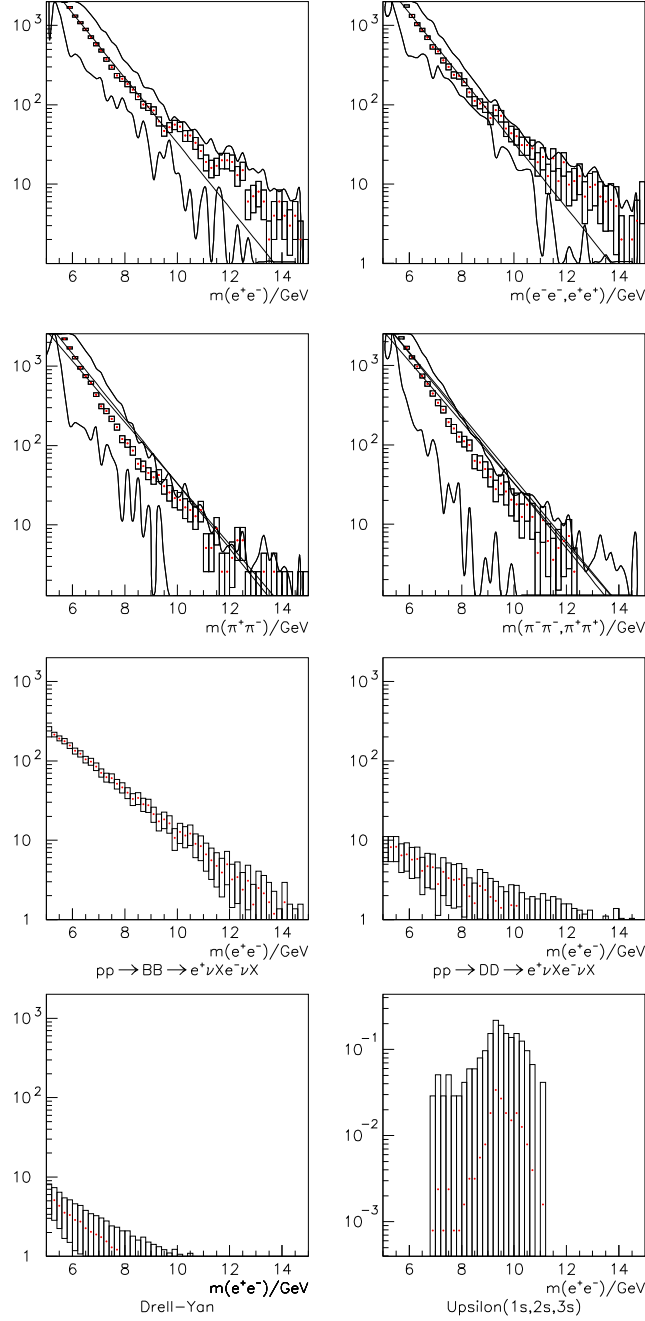


**Fig. 1.** Invariant mass for di-electrons and di-pions (control sample), for experimental data and PYTHIA 6.212. Statistical errors are shown as error bars, the white error band represents the systematic error. For details see Section 5. Please notice different y-axis scale by factor  $10^{-5}$  for  $\Upsilon$  (bottom, right).